

Series Expansions for Variable Electron Density

Weihong Zheng,^{*} C.J. Hamer,[†] and J. Oitmaa[‡]

School of Physics, The University of New South Wales, Sydney, NSW 2052, Australia.

R.R.P. Singh[§]

Department of Physics, University of California, Davis, CA95616, USA

(Dated: November 21, 2018)

Abstract

We have developed a series expansion method for calculating the zero-temperature properties of lattice electron models for variable electron density, i.e. for finite doping away from the half-filled case. This is done by introducing particle fluctuation terms in both the unperturbed Hamiltonian and perturbation. The method is demonstrated by application to the 2-chain $t - J$ ladder, where we provide comparison with previous work as well as obtaining a number of new results.

I. INTRODUCTION

The last 15 years have seen an explosion of interest in the study of lattice models of strongly correlated electrons. While, in large part, this has been driven by the field of high T_c superconductivity, there are other classes of materials whose properties are also determined by strong electron correlations, such as Kondo insulators, heavy fermion systems, and organic conductors.

Models for such systems usually start from the well known Hubbard and/or $t - J$ models, or generalizations of these. Exact solutions for these models are known only in 1-dimension. In higher dimensions, and indeed in 1-dimension for non-solvable cases, a variety of analytic and numerical techniques have been used: variational methods, exact diagonalizations for small systems, quantum Monte Carlo approaches, the density matrix renormalization group (DMRG), and perturbative “linked-cluster” series expansions. Yet it is well-known that strong-correlated electron models cause difficulties for most numerical techniques. Quantum Monte Carlo simulations are subject to the infamous “minus sign” problem, while exact diagonalization and DMRG calculations suffer from finite-size effects. It is therefore important to develop new techniques which may help to shed light on these problem.

In this paper we focus on series expansions at zero temperature¹. This approach has been used to study both the Hubbard model^{2,3} and the $t - J$ model^{4,5}. In the past this method has been restricted to states with one electron per site (half-filling) and to one and two-hole excitations away from half-filling. While this region of the phase diagram is itself of considerable interest, many of the more interesting aspects of strongly correlated systems occur for finite density of holes (“finite doping”).

We have explored a number of ways in which the series method might be adapted to

variable electron density and have been able to obtain consistent results for one model of considerable current interest, the $t - J$ ladder^{5,6,7}. The aim of this paper is thus twofold: to demonstrate the method, and to present new results for the $t - J$ ladder away from half-filling.

For completeness we summarize what is known for the $t - J$ ladder, both at half-filling and for finite doping. A clear discussion has been given by Troyer, Tsunetsugu and Rice⁸. At half-filling, and in the limit of strong interchain coupling, the ground state consists of spin singlet dimers on each rungs. The lowest spin excitation consists of a triplet excitation on one rung, propagating via the coupling between rungs. There are also quasiparticle excitations ($S = \frac{1}{2}$), corresponding in the limit to a hole excitation on a single rung –these carry both spin and charge, and separation of spin and charge does not occur in this model.

The lowest 2-hole excitation consists of a singlet hole pair on one rung, which develop into a band of states by propagation along the ladder. The zero-momentum state in this band is then the ground state in the 2-hole sector, and then the other states correspond to a gapless band of particle-hole charge excitations relative to the ground state. Correspondingly, the system is said to be in a C1S0) phase (1 gapless charge mode, 0 gapless spin modes).

A similar picture appear to hold as one moves away from the strong interchain coupling limit, even in the isotropic case which has been the object of most studies. As one moves away from half-filling, however, one finds that the lowest triplet excitation corresponds not to the simple triplet excitation of a singlet dimer, but to a particle-hole pair excitation on different rungs. Thus the triplet gap evolves discontinuously away from half-filling.⁸

Poilblanc, Scalapino and Hanke⁶ and Müller and Rice⁷ have presented a plausible phase diagram in the n versus J/t plane (for the isotropic case). For $J/t \lesssim 2$ the system is in a C1S0 phase (1 gapless charge mode) for low to moderate doping and crosses to a C1S1 phase (i.e. the spin-gap vanishes) for higher doping. For $J/t \gtrsim 2$ phase separation is predicted to

occur. For small J/t and low doping Müller and Rice⁷ also find ferromagnetic (Nagaoka) and C2S2 phases.

The paper is arranged as follows: in Sect. II we describe our series expansion method; Section III and IV present results, for a case with strong interaction coupling and for the isotropic case; Section IV gives a summary and discussion.

II. SERIES EXPANSIONS FOR VARIABLE ELECTRON DENSITY

The Hamiltonian of the $t - J$ ladder, in usual notation, is

$$\begin{aligned}
 H = & J \sum_{i,a} (\mathbf{S}_{i,a} \cdot \mathbf{S}_{i+1,a} - \frac{1}{4} n_{i,a} n_{i+1,a}) + J_{\perp} \sum_i (\mathbf{S}_{i,1} \cdot \mathbf{S}_{i,2} - \frac{1}{4} n_{i,1} n_{i,2}) \\
 & - t \sum_{i,a,\sigma} P(c_{i,a,\sigma}^{\dagger} c_{i+1,a,\sigma} + H.c.) P - t_{\perp} \sum_{i,\sigma} P(c_{i,1,\sigma}^{\dagger} c_{i,2,\sigma} + H.c.) P
 \end{aligned} \tag{1}$$

where i labels sites along each chain, σ ($=\uparrow$ or \downarrow) and a ($=1,2$) are spin and leg indices, P is a projection operator which excludes doubly occupied sites. J , t are exchange and hopping parameters on each chain, while J_{\perp} , t_{\perp} are coupling parameters between the two chains, i.e. on the rungs of the ladder.

In our previous work, and also in the present work, we employ a “rung basis”, in which the 2nd and 4th terms in (1) form the unperturbed Hamiltonian, and the remaining terms are treated perturbatively. The ground state of the unperturbed Hamiltonian, at half-filling, is then a direct product of spin-singlet states on each rung. Spin excitations, at half-filling, consist of a spin-triplet on one rung, which propagates coherently along the ladder. One and two-hole charge excitations are created by removing one or two electrons from a rung state and allowing these to propagate, via the t -hopping term.

At finite doping the situation is more complex, and it is impossible to identify a suitable unperturbed ground state. However it is possible to make progress by relaxing the con-

straint on particle number, by adding a particle nonconserving term to the Hamiltonian, and by introducing a chemical potential to control the electron density. A variety of particle nonconserving terms are possible, but we have found the following form

$$\frac{h}{\sqrt{2}} \sum_{i,a,\sigma} (c_{i,1,\uparrow}^\dagger c_{i,2,\downarrow}^\dagger - c_{i,1,\downarrow}^\dagger c_{i,2,\uparrow}^\dagger + H.c.),$$

to give best results. This term creates a spin-singlet on an empty rung or destroys a spin-singlet state to create an empty rung.

Our Hamiltonian, then, is

$$H = H_0 + xV \quad (2)$$

where

$$\begin{aligned} H_0 &= J_\perp \sum_i (\mathbf{S}_{i,1} \cdot \mathbf{S}_{i,2} - \frac{1}{4} n_{i,1} n_{i,2}) - t_\perp \sum_{i,\sigma} P(c_{i,1,\sigma}^\dagger c_{i,2,\sigma} + H.c.)P \\ &\quad + \frac{h}{\sqrt{2}} \sum_i P(c_{i,1,\uparrow}^\dagger c_{i,2,\downarrow}^\dagger - c_{i,1,\downarrow}^\dagger c_{i,2,\uparrow}^\dagger + H.c.)P - \mu \sum_i (n_{i,1} + n_{i,2}) \\ V &= J \sum_{i,a} (\mathbf{S}_{i,a} \cdot \mathbf{S}_{i+1,a} - \frac{1}{4} n_{i,a} n_{i+1,a}) - t \sum_{i,a,\sigma} P(c_{i,a,\sigma}^\dagger c_{i+1,a,\sigma} + H.c.)P \\ &\quad - \frac{h}{\sqrt{2}} \sum_i P(c_{i,1,\uparrow}^\dagger c_{i,2,\downarrow}^\dagger - c_{i,1,\downarrow}^\dagger c_{i,2,\uparrow}^\dagger + H.c.)P \end{aligned} \quad (3)$$

and x is an expansion parameter. The particle fluctuation term will mix sectors with different particle number, but these terms cancel in the physical limit $x = 1$, and the final results should be independent of the field h . In practice h can be adjusted to improve convergence for the extrapolation $x \rightarrow 1$. The electron density is determined by the chemical potential term, as usual.

The eigenstates of H_0 are direct products constructed from the nine possible rung states, which are given in Table I. For the range of parameters we use, the lowest energy rung state is

$$|\chi\rangle = (\kappa - J_\perp - 2\mu) |00\rangle - \sqrt{2}h(|\uparrow\downarrow\rangle - |\downarrow\uparrow\rangle) \quad (4)$$

where κ is defined in Table 1. This is a spin-singlet state.

To compute the perturbation series we choose values for the free parameters t, h, μ , and derive expansions in powers of x for the quantities of interest. Series have been computed to order x^{10} for the ground state energy E_0 , electron density n , and the dispersion relations for spin-triplet excitations $\Delta_s(k)$ and one-hole bonding excitations $\Delta_c(k)$. The calculations involve (trivial) 1-dimensional clusters up to 11 rungs, and are limited to this order by computer memory constraints. The series are then evaluated at $x = 1$, corresponding to the full Hamiltonian, by integrated differential approximants⁹. The series are too numerous to be reproduced here, but are available on request.

III. RESULTS FOR THE DOPED $T - J$ LADDER (STRONG RUNGS)

As our series expansion is about the rung limit, convergence will naturally be better when the rung coupling terms are greater than coupling along the chains. We present in this Section results for $J_\perp/J = 4$.

We first consider the ground state energy as a function of chemical potential μ . We have evaluated series, in powers of x to order x^{10} , for various fixed h, μ . The leading terms are

$$E_0/N = -\frac{1}{4}(J_\perp + 2\mu + \kappa) + x\left(\frac{h^2}{\kappa} - \frac{(J_\perp + 2\mu + \kappa)^2}{16\kappa^2}J\right) + O(x^2) \quad (5)$$

with $\kappa = \sqrt{4h^2 + (J_\perp + 2\mu)^2}$. Figure 1 shows curves of E_0 versus μ for $t = J = 0.25$, $t_\perp = J_\perp = 1$. The solid line in this figure is the result for half-filling ($n = 1$). For this case the charge degrees of freedom are frozen out, and the system is equivalent to a Heisenberg spin ladder, where the ground state energy per site, for $J_\perp = 4J$, is $E_0/NJ_\perp = -0.38803708$ ¹⁰. Including the other terms gives, at half-filling, $E_0/NJ = -0.38803708 - 3/16 - \mu$, which is the solid line in the figure. For $\mu \gtrsim 0.05$ our ground state energy is very close to that

for half-filling. If we take a large value of μ , $\mu = 5$, to make sure the system is half-filled at $x = 1$, the ground state energy is estimated to be $E_0/NJ_\perp = -5.575537(1)$, which agrees with the results for the Heisenberg spin ladder to 6 digits. The results in Figure 1 have been obtained by adjusting the field h to obtain best convergence. An illustration of the sensitivity of this procedure is shown in Figure 2, where E_0 is plotted versus h , for $J_\perp = t_\perp = 1$, $J = t = 0.25$, and $\mu = 0.08$. The size of the error bars, which represent the spread among different approximants, is least for $h \sim 0.25$, which is the value used. E_0 itself is relatively insensitive to the value of h chosen.

The electron density is obtained via the standard relation

$$n = -\frac{\partial E_0}{\partial \mu N} \quad (6)$$

from which we obtain series in x , which are again evaluated at $x = 1$ via approximants. Figure 3 shows curves of electron density versus μ for the same parameters as Fig. 1. Half-filling corresponds to large μ , as expected. As μ decreases, the electron density begins to drop, and below $\mu \simeq 0$ the error bars increase substantially, but the overall trend is very clear.

We have used the data of Figures 1 and 3 to compute the ground state energy as a function of n , and this is shown in Figure 4. In this figure we have subtracted the chemical potential term μn from the energy. The ground state energy seems rather insensitive to the electron density from these parameters.

Next we consider the dispersion relation $\Delta_s(k)$ for triplet spin excitations. At half-filling these excitations correspond physically to a triplet excitation on a rung propagating coherently along the ladder. At finite doping the situation is more complicated because rung singlets contain an admixture of empty states, and singlet-triplet excitation processes include pair creation terms. Nevertheless spin-triplet excitations are well defined and their

energy dispersion can be calculated via series methods^{1,11}. Figure 5 shows the triplet spin dispersion curve $\Delta_s(k)$ for $J_\perp = t_\perp = 1$, $J = t = 0.25$, and $\mu = 5, 0.15, 0.08, 0.025$, which correspond to $n = 1.000000(1), 0.99(1), 0.90(1), 0.80(2)$, respectively. For $\mu = 5$, the system is at half-filling, and we can reproduce the dispersion curve for the Heisenberg spin ladder with $4J = J_\perp$ ¹⁰, up to 6 digits. The figure shows that the triplet dispersion is very sensitive to doping, with a significant change already for 1% doping ($\mu = 0.15$). The minimum triplet gap remains at $k = \pi$ for low doping ($n \gtrsim 0.8$). The size of the gap decreases for very low doping, but then begins to increase. By $n = 0.8$ the dispersion curve has become quite flat near the zone boundary, and it appears that the minimum triplet energy shifts to intermediate k values for larger doping.

IV. RESULTS FOR THE DOPED $T - J$ LADDER (ISOTROPIC CASE)

Most previous studies of the $t - J$ ladder have been for the isotropic exchange case $J = J_\perp$, $t = t_\perp$. Although our series here are less regular we are able to obtain results which can be compared to previous work. We follow, more or less, the order of Section III.

Figure 6 shows curves of E_0 versus μ for $t = 0.46, 0.55, 0.75, 1.0$. The solid line in this figure is the result for half-filling ($n = 1$) where the ground state energy per site, for $J = J_\perp$, is $E_0/NJ = -0.578043 - 3/8 - \mu$.¹⁰ For $\mu \gtrsim 0.1-0.2$ our ground state energy is very close to that for half-filling, for all t considered.

Figure 7 shows curves of electron density versus μ for $t = 0.55, 0.75, 1, 2$ (setting $J = 1$). For $\mu \gtrsim -0.7$ the electron density decreases with increasing t , for constant μ ; or equivalently for fixed n the value of μ increases with t . Around $\mu \simeq -0.8$ there is a crossover region where the value of n is insensitive to t , and below this value of μ the dependence of n on t is the opposite to that discussed above. As t decreases the curves of n versus μ steepen,

and at the critical point for phase separation, estimated to be $t_c = 0.4638^{12}$, we expect a discontinuous drop away from $n = 1$ to develop at some critical separation value μ_c . Our series data are not currently expressed as analytical functions of μ , and do not allow us to explore the phase separation phenomenon any further here.

We have used the data of Figure 7 to compute the ground state energy as a function of n , and these results are shown in Figure 8. For ease of comparison with previous work we have subtracted the chemical potential term μn from the energy. Figure 8 also serves to compare our results with previous work. The filled circles at $n = 0.5$ are our previous results⁵ for quarter-filling, for $t = 0.55, 0.75, 1.0$. The dashed and solid lines are results obtained from a hard-core boson approximation (HCB) and a recurrence-relation method (RRM) for $t = 2$ by Sierra *et al.*¹³ The crosses are Density Matrix Renormalization Group results¹³, also for $t = 2$. The latter agree very well with our series estimates, whereas the analytic approximations clearly give too high an energy.

Next we consider the dispersion relation $\Delta_s(k)$ for triplet spin excitations. Figure 9 shows the triplet spin dispersion curve $\Delta_s(k)$ for $t = 0.75$, and $\mu = 5, 0.1, -0.1, -0.45, -0.85$ which correspond to $n = 1.000(2), 0.99(3), 0.91(3), 0.61(3), 0.47(4)$, respectively. The solid curve is the dispersion curve for the Heisenberg spin ladder with $J = J_\perp$ ¹⁰. This is the dispersion curve for half-filling, and agrees very well with the present results for $\mu = 5$. The figure again shows that the triplet dispersion is very sensitive to doping, with a significant change already for 1% doping ($\mu = 0.1$). At small doping the minimum triplet energy remains at $k = \pi$, as for half-filling, but for large doping it shifts to intermediate k values. The series become more irregular and the error bars are correspondingly larger. For $\mu = -0.85$, the shift in the minimum energy has become a dramatic effect.

Figure 10 shows the triplet spin dispersion curve $\Delta_s(k)$ for $t = 0.55, 0.75, 1$ and 2 , and

μ is chosen to be -0.54, -0.24, 0.14, 1.9 respectively, so that $n \simeq 0.8$. We also show, in the Figure, previous results for the minimum energy gap obtained from exact diagonalizations by Hayward *et al.*¹⁴ As can be seen, the agreement is excellent.

Finally we turn to charge excitations, in particular the 1-hole bonding excitation (which couples rung states 1 and 6, or 1 and 7 in Table 1). These excitations correspond to creation or destruction of a hole in the ground state. Figure 11 show the dispersion $\Delta_c(k)$, again for $t = 0.75$ and various μ , together with the corresponding dispersion curve for the Heisenberg spin ladder (solid line)⁴. This curve, which corresponds to half-filling, again agrees very well with our present results for $\mu = 5$. A small amount of doping (up to 10%) has little effect on the dispersion curve for $k \lesssim \pi/2$, but results in a noticeable flattening for larger k . For $\mu = -0.45$ (corresponding to $n \simeq 0.6$) there is a pronounced minimum at $k \simeq \pi/2$ and a large increase in excitation energy for larger k . Troyer *et al.* have previously noted this substantial shift in the minimum of the dispersion curve for the bonding and antibonding bands, and have identified the minima with the Fermi points of the respective quasiparticle bands.

V. DISCUSSION AND SUMMARY

The method of linked-cluster perturbation expansions for strongly interacting lattice electron models has, until now, been restricted to systems with one electron per site (half-filling) or to one or two holes in the half-filling state. In this paper we show, for the first time, how this constraint can be relaxed, and we demonstrate its reliability in the case of the 2-leg $t - J$ ladder, where comparisons with other methods can be made. The agreement is found to be well within the error estimates.

We present a number of new results for the $t - J$ ladder, for the ground state energy

and electron density as functions of chemical potential, and for the ground state energy and some excitation energies for different values of electron density. Results are presented for a case in which the rung interactions are stronger than the chain interactions (by a factor of 4) and also for the isotropic case.

This work opens up new possibilities for exploring other aspects of strongly correlated electron models with a finite hole density, and we intend to take up some of these in future work. The series approach is not subject to finite-size effects, unlike exact diagonalization, the DMRG, or (to a lesser extent) Monte Carlo simulations; and it provides a versatile complementary method to these other numerical techniques. It also suffers from some limitations, of course, for instance, it does not allow one to explore the phase separated regime, where the electron density dependence on the chemical potential is discontinuous.

Acknowledgments

The work of Z.W., C.J.H. and J.O. forms part of a research project supported by a grant from the Australian Research Council, R.R.P.S. is supported in part by NSF grant number DMR-9986948. We have benefited from discussions with Professor O.P. Sushkov. The computation has been performed on the AlphaServer SC computer. We are grateful for the computing resources provided by the Australian Partnership for Advanced Computing (APAC) National Facility.

* w.zheng@unsw.edu.au; <http://www.phys.unsw.edu.au/~zwh>

† c.hamer@unsw.edu.au

‡ j.oitmaa@unsw.edu.au

§ singh@raman.ucdavis.edu

¹ M.P. Gelfand and R.R.P. Singh, *Adv. Phys.* **49**, 93(2000).

² Z.P. Shi and R.R.P. Singh, *Phys. Rev. B* **52**, 9620(1995); *Europhys. Lett.* **3**, 219(1995).

³ W. Zheng, J. Oitmaa, C.J. Hamer and R.J. Bursill, *J. Phys. Condens. Matter* **13**, 433(2001).

⁴ C.J. Hamer, W.H. Zheng, and J. Oitmaa, *Phys. Rev. B* **58**, 15508 (1998).

⁵ J. Oitmaa, C.J. Hamer and W.H. Zheng, *Phys. Rev. B* **60**, 16364(1999).

⁶ D. Poilblanc, D.J. Scalapino and W. Hanke, *Phys. Rev. B* **52**, 6796(1995).

⁷ T.F.A. Müller and T.M. Rice, *Phys. Rev. B* **58**, 3425(1998).

⁸ M. Troyer, H. Tsunetsugu and T.M. Rice, *Phys. Rev. B* **53**, 251(1996).

⁹ A.J. Guttmann, in “Phase Transitions and Critical Phenomena”, Vol. 13 ed. C. Domb and J. Lebowitz (New York, Academic, 1989).

¹⁰ W.H. Zheng, V. Kotov, and J. Oitmaa, *Phys. Rev. B* **57**, 11439 (1998).

¹¹ M.P. Gelfand, *Solid State Commun.* **98**, 11(1996).

¹² S. Rommer, S.R. White and D.J. Scalapino, *Phys. Rev. B* **61**, 13424(2000).

¹³ G. Sierra, M.A. Martin-Delgado, J. Dukelsky, S.R. White, and D.J. Scalapino, *Phys. Rev. B* **57**, 11666(1998).

¹⁴ C.A. Hayward, D. Poilblanc, and D.J. Scalapino, *Phys. Rev. B* **53**, R8863(1996)

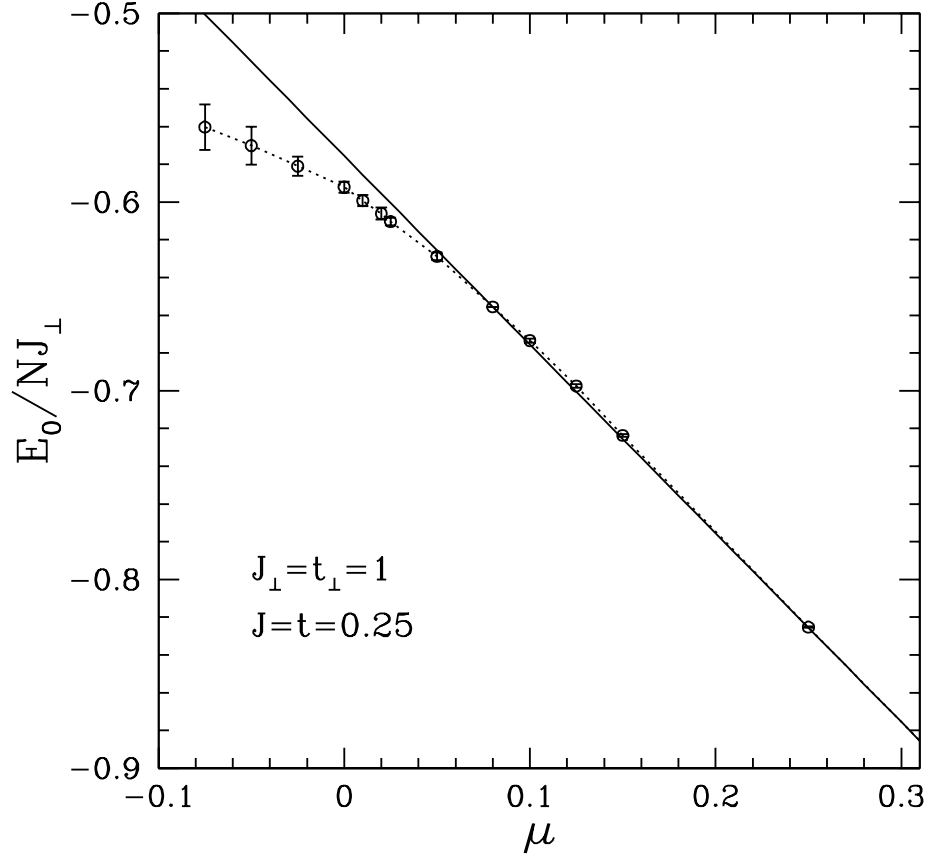


FIG. 1: The ground state energy per site E_0/NJ versus μ for $J_{\perp} = t_{\perp} = 1$, $J = t = 0.25$. The solid line is the result at half-filling¹⁰.

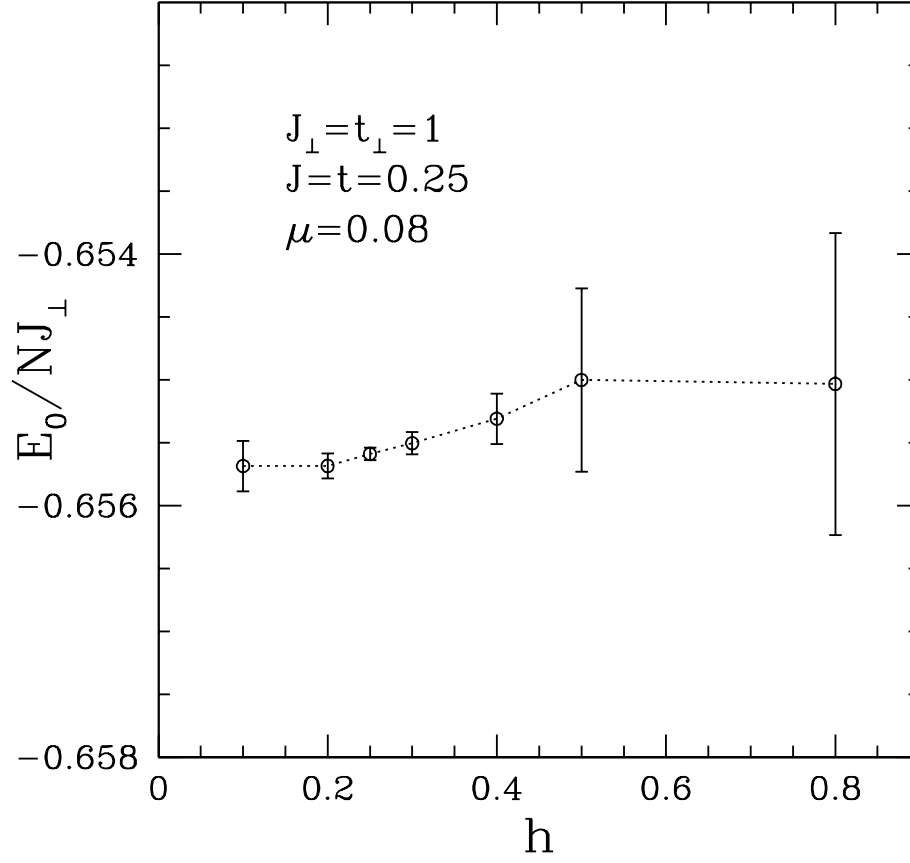


FIG. 2: The ground state energy per site E_0/NJ versus h for $J_{\perp} = t_{\perp} = 1$, $J = t = 0.25$, and $\mu = 0.08$.

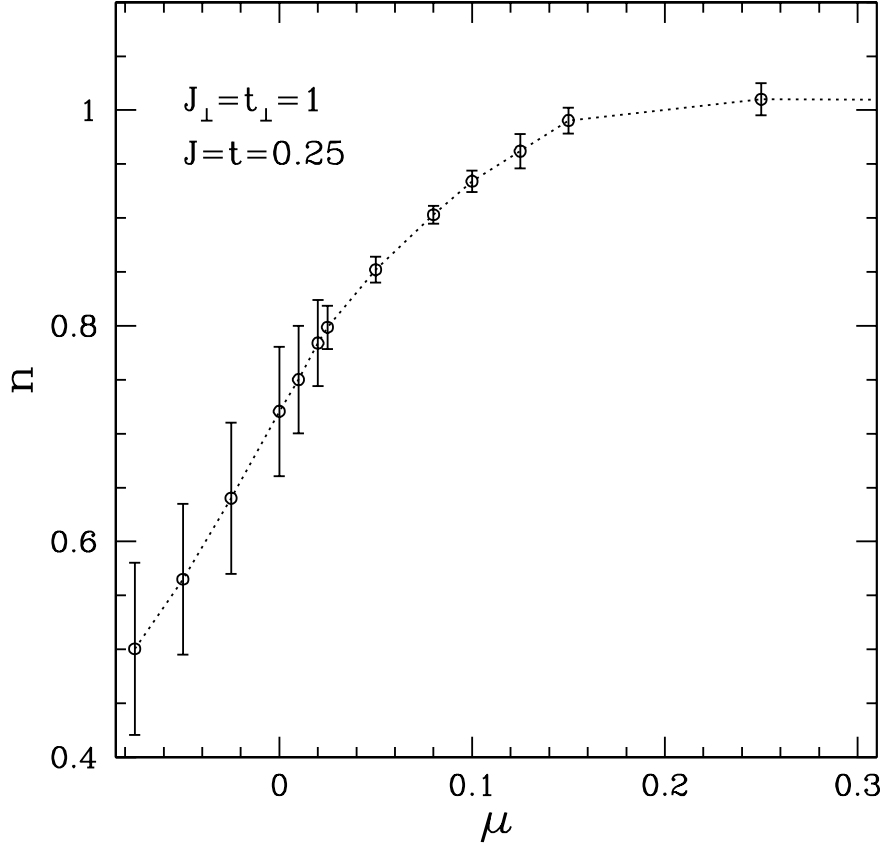


FIG. 3: The electron density n versus μ for $J_{\perp} = t_{\perp} = 1$, $J = t = 0.25$.

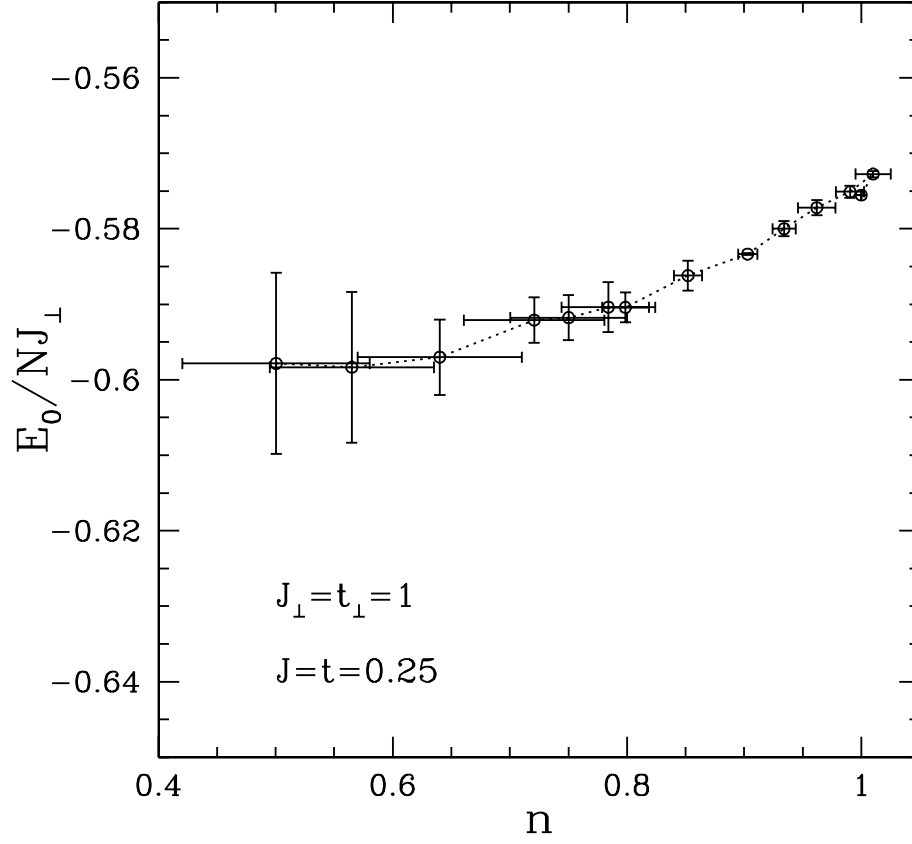


FIG. 4: The ground state energy versus electron density n for $J_{\perp} = t_{\perp} = 1$, $J = t = 0.25$.

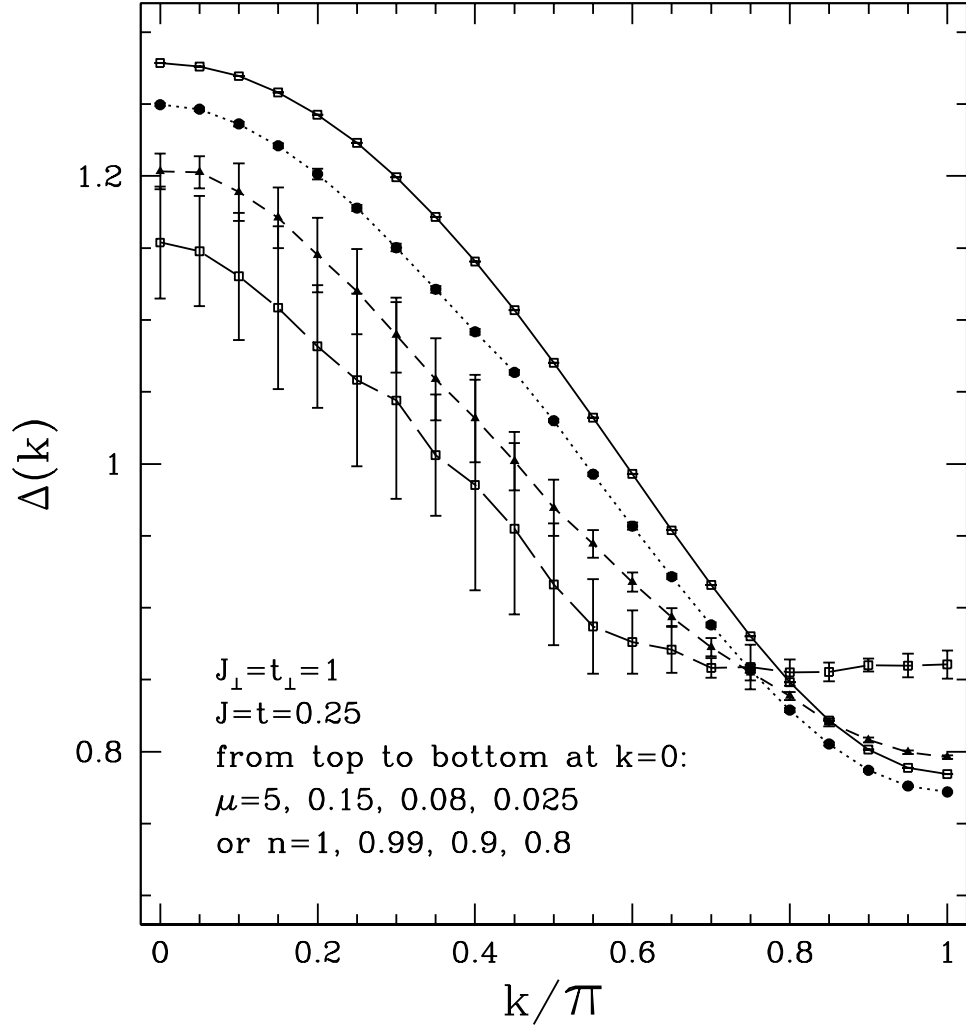


FIG. 5: The triplet spin dispersion relation for $J_{\perp} = t_{\perp} = 1$, $J = t = 0.25$ and $\mu = 5, 0.15, 0.08, 0.025$, corresponding to $n = 1, 0.99, 0.9, 0.8$.

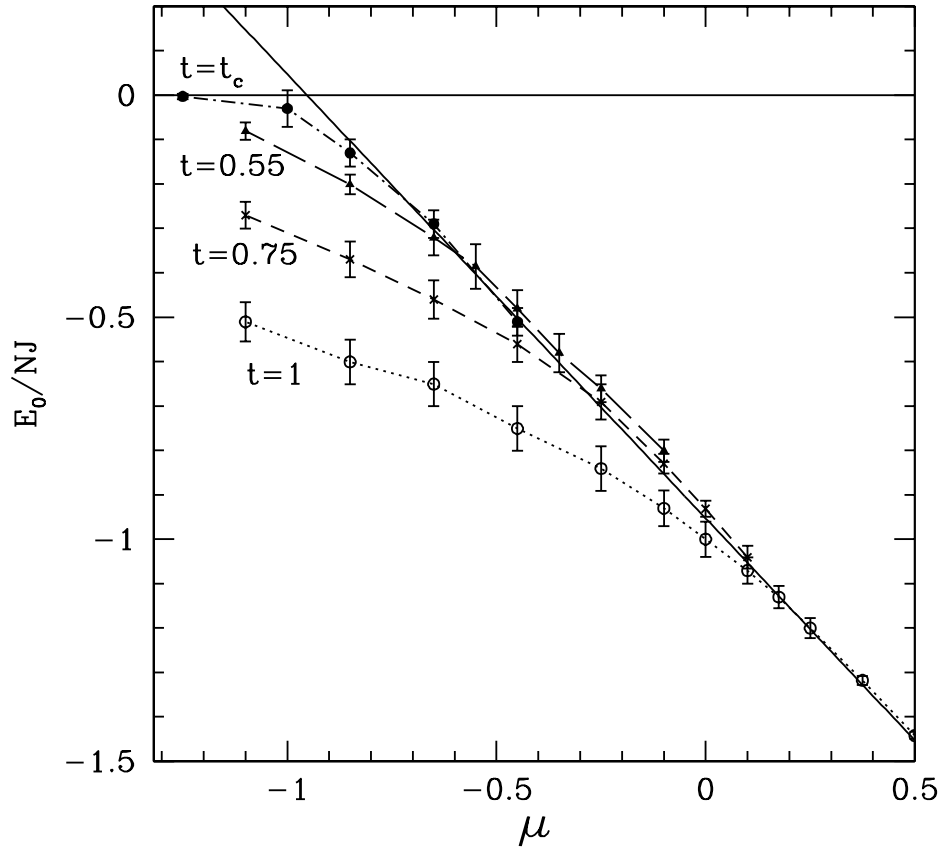


FIG. 6: The ground state energy per site E_0/NJ versus μ for $t = 0.4638, 0.55, 0.75$ and 1 . The solid line is the result at half-filling¹⁰.

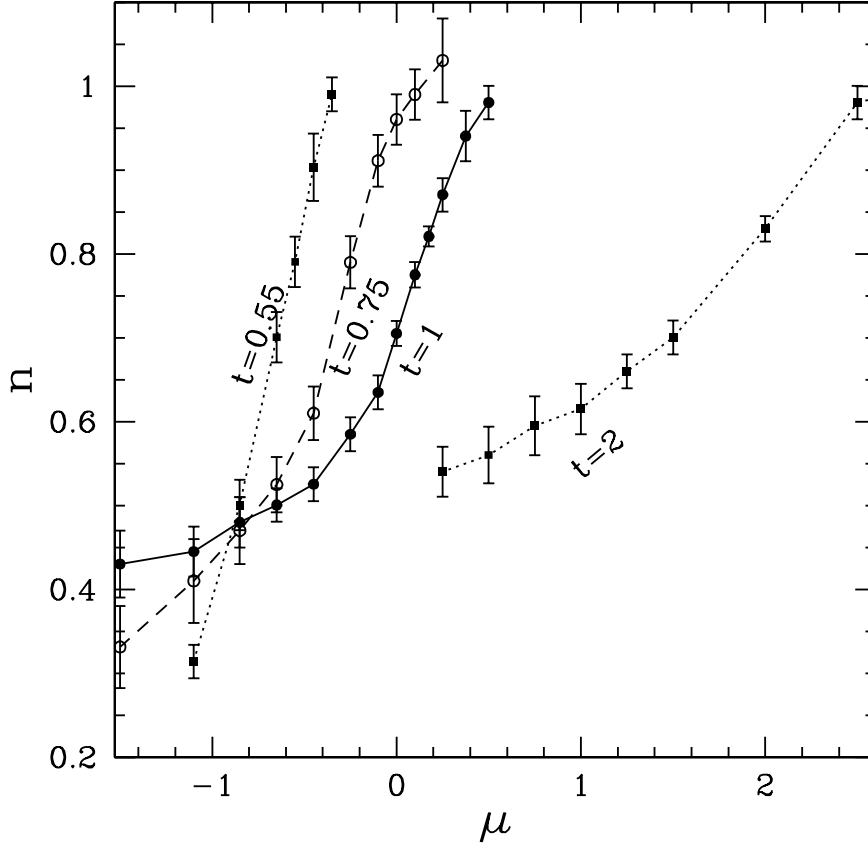


FIG. 7: The electron density n versus μ for $t = 0.55, 0.75, 1$ and 2 .

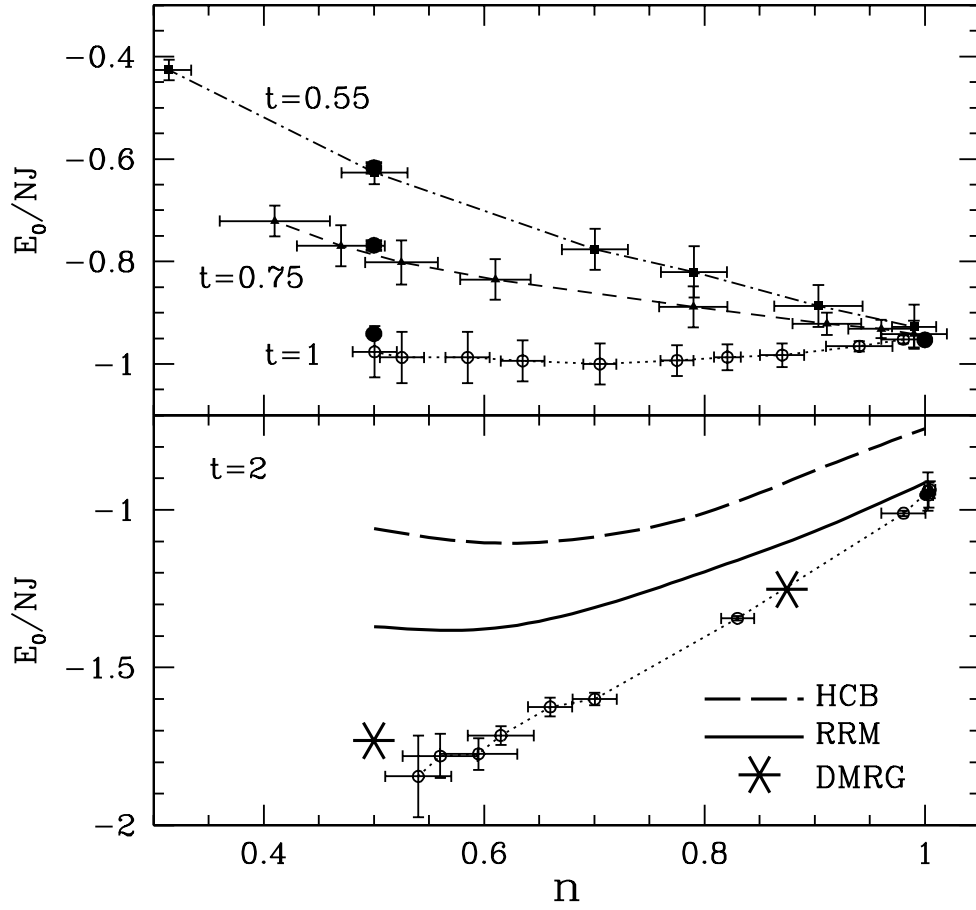


FIG. 8: The ground state energy versus electron density n for $t = 0.55$, 0.75 , 1 (upper window) and 2 (lower window). The large solid circles at quarter filling and half-filling are the results of series expansions at quarter filling⁵ (for $t = 0.55$, 0.75 and 1) and series expansions for the Heisenberg ladder¹⁰. The bold long dashed line, solid line and stars are the results of HCB, RRM and DMRG¹³ for $t = 2$.

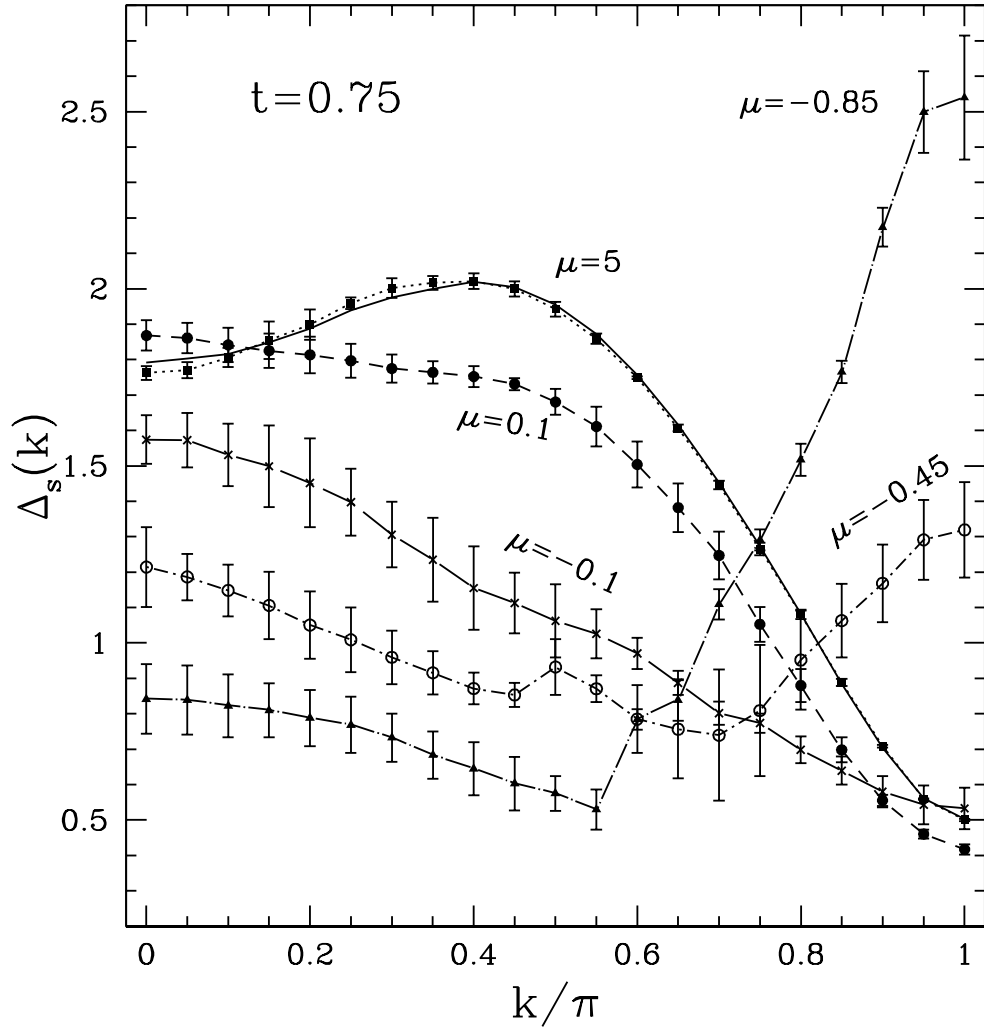


FIG. 9: The triplet spin dispersion relation for $t = 0.75$ and different μ . Also presented are results for the Heisenberg spin ladder for $J = J_{\perp}$ (solid line)¹⁰.

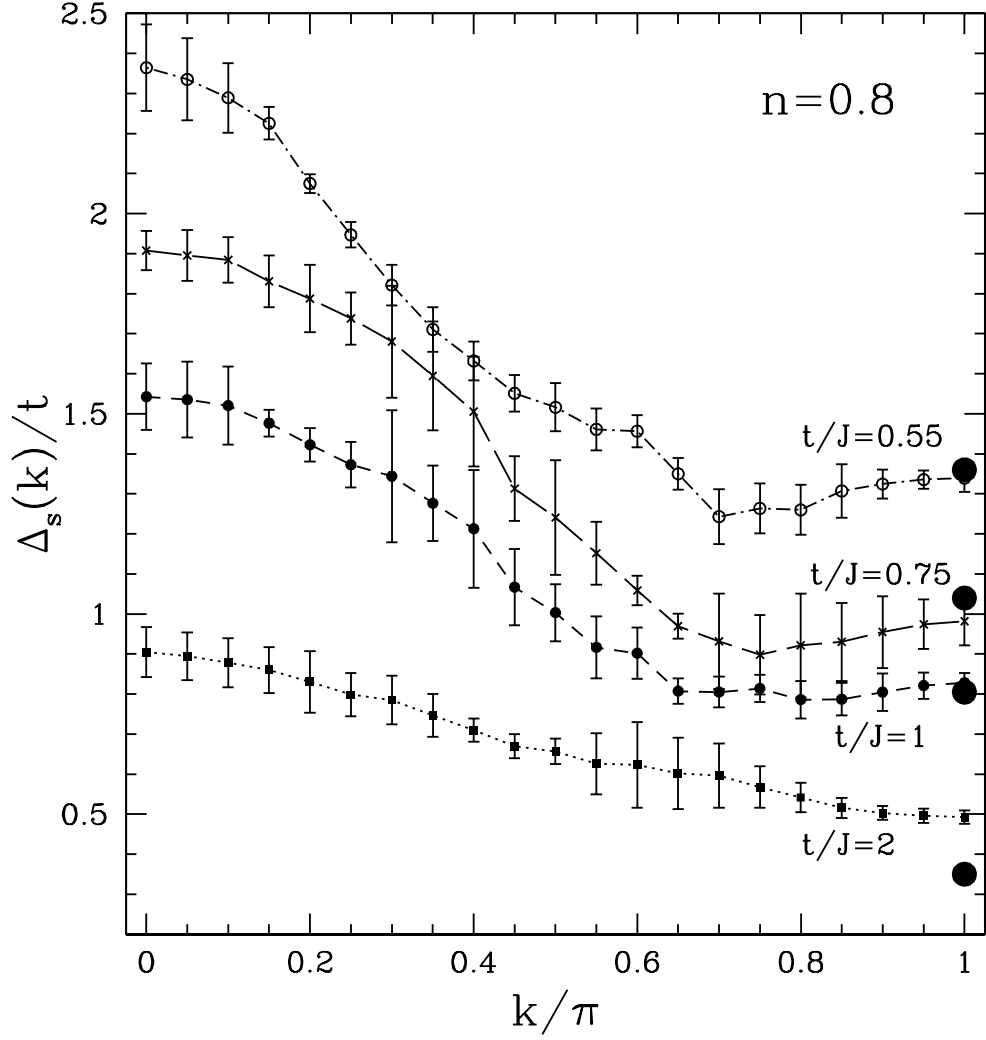


FIG. 10: The triplet spin dispersion relation for $t/J = 0.55, 0.75, 1$ and 2 and $n = 0.8$. The full solid points are the finite lattice results for the minimum gap [Ref. 14].

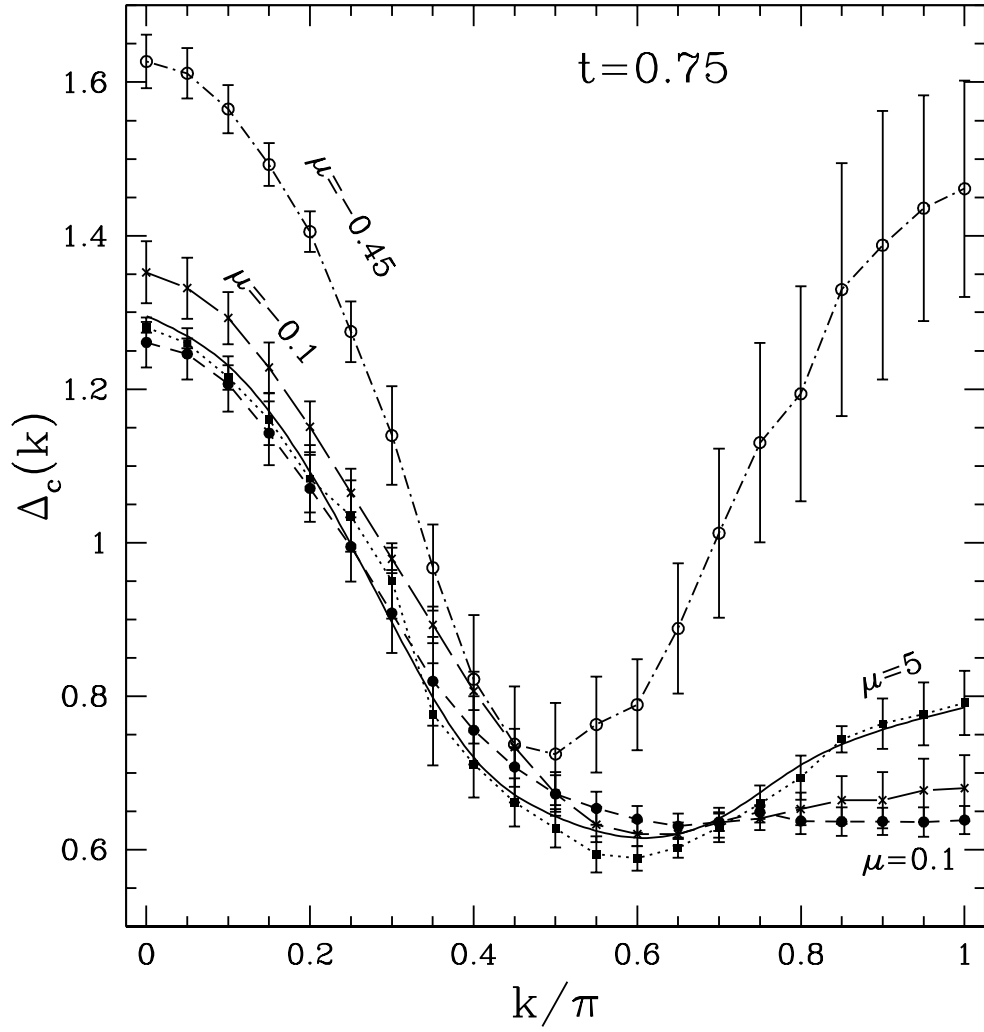


FIG. 11: The dispersion relation for the one-hole bonding excitation at $t = 0.75$ and different μ .

Also presented are the results at half-filling (solid line)⁴.

TABLE I: The nine rung states and their energies, where $\kappa = \sqrt{4h^2 + (J_\perp + 2\mu)^2}$.

No.	Eigenstate	Eigenvalue	Name
1	$(\kappa - J_\perp - 2\mu) 00\rangle - \sqrt{2}h(\uparrow\downarrow\rangle - \downarrow\uparrow\rangle)$	$-(J_\perp + 2\mu + \kappa)/2$	lower energy singlet
2	$ \downarrow\downarrow\rangle$	-2μ	triplet ($S_{\text{tot}}^z = -1$)
3	$\frac{1}{\sqrt{2}}(\uparrow\downarrow\rangle + \downarrow\uparrow\rangle)$	-2μ	triplet ($S_{\text{tot}}^z = 0$)
4	$ \uparrow\uparrow\rangle$	-2μ	triplet ($S_{\text{tot}}^z = 1$)
5	$-(J_\perp + \kappa + 2\mu) 00\rangle - \sqrt{2}h(\uparrow\downarrow\rangle - \downarrow\uparrow\rangle)$	$(\kappa - J_\perp - 2\mu)/2$	higher energy singlet
6	$\frac{1}{\sqrt{2}}(0\downarrow\rangle + \downarrow0\rangle)$	$-t_\perp - \mu$	electron-hole bonding ($S_{\text{tot}}^z = -\frac{1}{2}$)
7	$\frac{1}{\sqrt{2}}(0\uparrow\rangle + \uparrow0\rangle)$	$-t_\perp - \mu$	electron-hole bonding ($S_{\text{tot}}^z = \frac{1}{2}$)
8	$\frac{1}{\sqrt{2}}(0\downarrow\rangle - \downarrow0\rangle)$	$t_\perp - \mu$	electron-hole antibonding ($S_{\text{tot}}^z = -\frac{1}{2}$)
9	$\frac{1}{\sqrt{2}}(0\uparrow\rangle - \uparrow0\rangle)$	$t_\perp - \mu$	electron-hole antibonding ($S_{\text{tot}}^z = \frac{1}{2}$)